

# High performance and compact $1 \times 3$ beam splitter based on parallel silicon waveguide

Junbo Yang (杨俊波)<sup>1,2\*</sup>, Suzhi Xu (徐素芝)<sup>1</sup>, Kuo Zhou (周 阔)<sup>1</sup>, and Jia Xu (徐 佳)<sup>1</sup>

<sup>1</sup>Center of Material Science, National University of Defense Technology, Changsha 410073, China

<sup>2</sup>State Key Laboratory on Advanced Optical Communication Systems and Networks, Peking University, Beijing 100871, China

\*Corresponding author: yangjunbo008@sohu.com

Received August 02, 2013; accepted October 19, 2013; posted online March 20, 2014

We propose a novel and compact broadband  $1 \times 3$  beam splitter (BS), which is based on optical tunneling between neighbor and parallel waveguides; thus, it is used to couple energy from one waveguide to another. This device consists of three parallel planar waveguides, in which the energy is transferred in a coherent fashion, so that the direction of propagation is maintained. For complete energy transfer to occur between the neighbor waveguides, they must have identical propagation constants. Thus, indices and height of the waveguide layers are controlled very carefully to provide matching propagation constants. The total length of BS is only about  $7 \mu\text{m}$ . The simulation and analysis show that the BS for transverse magnetic (TM) light at a wavelength of  $1.55 \mu\text{m}$  is designed to split incident light into three beams, whose power is 20, 34, and 18%, respectively. The wavelength bandwidth reaches up to  $52 \text{ nm}$  with an increase in wavelength from  $1.49$  to  $1.542 \mu\text{m}$ , in which the maximum power difference of three output ports is less than 10%; moreover, the minimum is nearly 0. BS designed here particularly suits for optical communication and optical information processing.

OCIS codes: 050.6624, 060.4510, 130.4815, 230.3990.  
doi: 10.3788/COL201412.S10501.

Beam splitter (BS) is a fundamental optical component used in optical instruments and scientific research, which has many optical information-processing applications, such as free-space optical switching network, read-write magneto-optical data-storage systems, and polarization-based imaging systems. Functionality of a conventional BS has been based on natural birefringent effects (e.g., Thomson prisms, Nicol prisms, and Wollaston prisms), the refraction effect at multilayered dielectric coatings, the absorption effect of a dichroic polarizer, the diffraction effect of grating structures, or a combination of several of these effects, which are bulky, heavy, and expensive and not suitable for integrated optical circuits.

Recently, many researchers are interested to use micro/nano structure to realize beam splitting due to its inherent advantages, including compact size, low loss, and easy to integrate with other devices<sup>[1-3]</sup>, which include grating structure design, photonic crystal design, and surface plasmon polaritons (SPPs), etc. For example, a  $1 \times 3$  BS for transverse electric (TE) polarization was designed, fabricated and characterized based on inspiration from multimode interference self-imaging phenomena in photonic crystal waveguides<sup>[4]</sup>. Similarly, a self-collimation-based directional emitter and BS are presented in a two-dimensional photonic crystal<sup>[5]</sup>. Zhang and Armani, in their study, have reported a  $2 \times 2$  suspended silica splitter integrated on a silicon substrate<sup>[6]</sup>. More recently, the tunable metal-insulator-metal plasmonic power splitter based on excitation of SPPs has also been analyzed<sup>[7]</sup>. Obviously, these designs are rather complicated and difficult to fabricate, which limit the application in an optical communication field due to high cost and power loss.

In this paper, we are concerned on the traditional waveguide directional coupler for  $1 \times 3$  BS. This splitter is designed for a wavelength of  $1.55 \mu\text{m}$  under TM polarization. The length of the structure is only  $7 \mu\text{m}$ , and the finite-difference time-domain (FDTD) method, a powerful and accurate method for finite-size structure, is chosen to simulate and design this splitter.

Figure 1 shows a proposed BS structure which is simple and composed of three parallel silicon waveguides (the length of  $L_1 = 3 \mu\text{m}$ ) on a silica layer with a gap of  $40 \text{ nm}$  between neighbor parallel waveguides, and a tree-shaped silicon waveguide including three output ports with the length of  $L_2 = 4 \mu\text{m}$ . Thus, the total length of  $1 \times 3$  BS is about  $7 \mu\text{m}$ . Simultaneously, the height  $h$  and the width  $w$  of silicon waveguide are  $220$  and  $300 \text{ nm}$ , respectively. The spacing  $t$  between the neighbor output ports is  $2 \mu\text{m}$ .

The optical tunneling phenomenon can be used to couple energy from one waveguide to another. Couplers of this type are usually called directional couplers because the energy is transferred in a coherent fashion

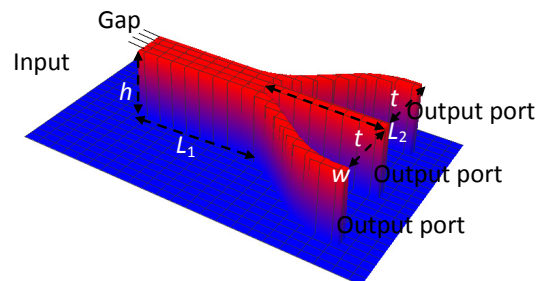


Fig. 1. Schematic layout of  $1 \times 3$  beam splitter.

so that the direction of propagation is maintained. Primarily, the dual-channel directional coupler is discussed (Fig. 2).

A concise theory of operation of the dual-channel directional coupler can be developed by following the coupled mode theory approach of Yariv<sup>[8-12]</sup>. The coupling between modes is given by general coupled-mode equations for amplitudes of the two modes. Thus,

$$\frac{dA_0(z)}{dz} = -i\beta_0 A_0(z) + \kappa_{01} A_1(z), \quad (1)$$

$$\frac{dA_1(z)}{dz} = -i\beta_1 A_1(z) + \kappa_{10} A_0(z), \quad (2)$$

where,  $A(z)$  is a complex amplitude which includes the phase term  $\exp(-i\beta z)$ ;  $\beta_0$  and  $\beta_1$  are the propagation constants of the modes in the two guides; and  $\kappa_{01}$  and  $\kappa_{10}$  are the coupling coefficients between modes. Consider the guides shown in Fig. 2; and assume that the guides are identical and that they both have an exponential optical loss coefficient  $\alpha$ . Thus,  $\beta = \beta_r - i\frac{\alpha}{2}$ , where,  $\beta = \beta_0 = \beta_1$ , and  $\beta_r$  is the real part of  $\beta$ . In case of identical guides, it is obvious from reciprocity that  $\kappa_{01} = \kappa_{10} = -i\kappa$ , where  $\kappa$  is real. Thus, the power flow in the guides is given by

$$P_0(z) = A_0(z)A_0^*(z) = \cos^2(\kappa z)e^{-\alpha z}, \quad (3)$$

$$\text{And, } P_1(z) = A_1(z)A_1^*(z) = \sin^2(\kappa z)e^{-\alpha z}, \quad (4)$$

From Eqs. (3) and (4), it can be observed that the power does indeed transfer back and forth between the two guides as a function of length. The length  $T$  necessary for complete transfer of power from one guide to the other is given by

$$T = \frac{\pi}{2\kappa} + \frac{m\pi}{\kappa}, \quad (5)$$

where,  $m = 0, 1, 2, \dots$ . In a real guide, with absorption and scattering losses,  $\beta$  is complex. Hence, the total power contained in both the guides decreases by a factor  $\exp(-\alpha z)$ .

Using FDTD method, Figs. 3(a) and (b) indicate the magnitude of Poynting vector distribution of TE polarization and TM polarization, respectively, and their corresponding wave profiles in silicon waveguide are also shown in Figs. 4(a) and (b).

The oscillations indicate obviously the energy transfer between the two adjacent silicon waveguides, in

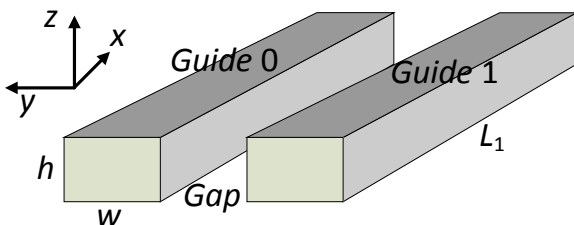


Fig. 2. Dual-channel directional coupler.

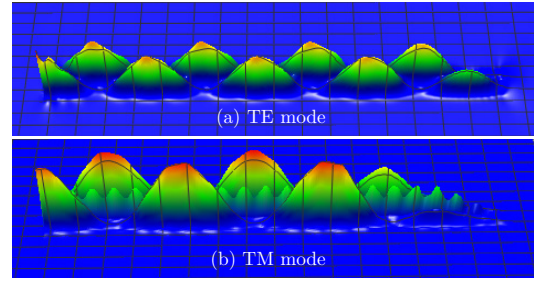


Fig. 3. Magnitude distribution of Poynting vector for a dual-waveguide coupler.

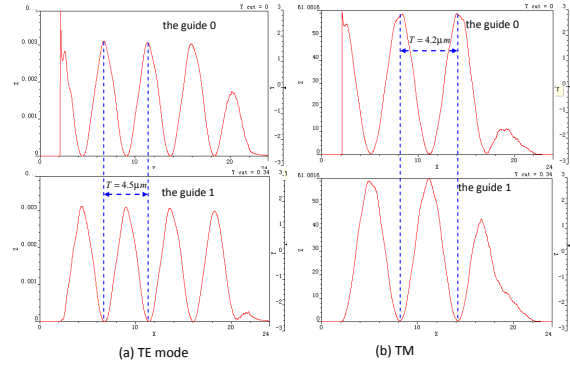


Fig. 4. Wave profile in silicon waveguide.

which the oscillation period  $T$  values of the TE and TM modes are about 4.5 and 4.2  $\mu\text{m}$ , respectively, and very close to each other. According to the above discussion, the relationship between the gaps, the width of waveguide, wavelength, and the oscillation period is analyzed, respectively, as shown in Figs. 5(a), (b), and (c).

Obviously, the oscillation period values of TE and TM modes are very close to each other when the following conditions are met:

$$\begin{aligned} 40\text{nm} &\leq \text{Gap} \leq 50\text{nm}, 1.54\mu\text{m} \leq \lambda \leq 1.55\mu\text{m}, \\ 200\text{nm} &\leq w \leq 320\text{nm}. \end{aligned}$$

The  $1 \times 3$  BS is discussed and analyzed in further sections based on the above design parameters. According to the dual-waveguide directional coupler, the three-waveguide directional coupler is also proposed (Fig. 6). The beams which incident from the input port of the middle waveguide are coupled with two adjacent waveguides based on above analysis. Thus, the total power transmitted along the input waveguide is separated into three parts with appropriate design parameters.

Figures 7(a) and (b) indicate the magnitude of Poynting vector distribution of TE polarization and TM polarization, respectively. Their corresponding wave profiles in silicon waveguide are also shown in Figs. 8(a) and (b), respectively.

As discussed above, the oscillations also indicate the energy transfer among the three adjacent silicon waveguides, in which the period values of the TE and TM modes are about 3.4 and 4.5  $\mu\text{m}$ , respectively. In addition, the simulation results show that the power

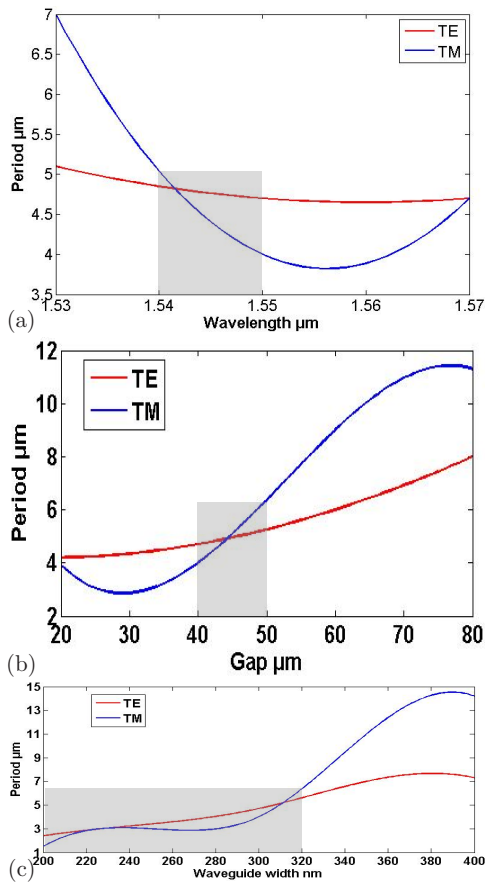


Fig. 5. The relationship between the gap, the width of waveguide, wavelength, and the period. (a) Period as a function of gap with wavelength 1.55 μm, height 220 nm, and width 300 nm. (b) Period as a function of wavelength, gap = 40nm, height = 220nm, and width = 300nm (c) Period as a function of waveguide width with gap of 40 nm, wavelength of 1.55 μm and height of 220 nm.

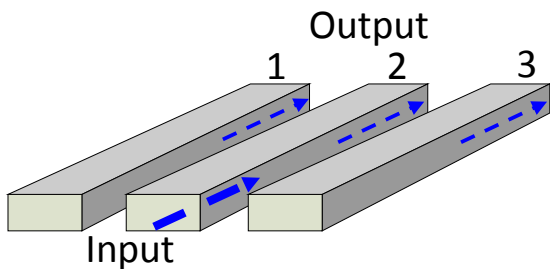


Fig. 6. Three parallel planar waveguides.

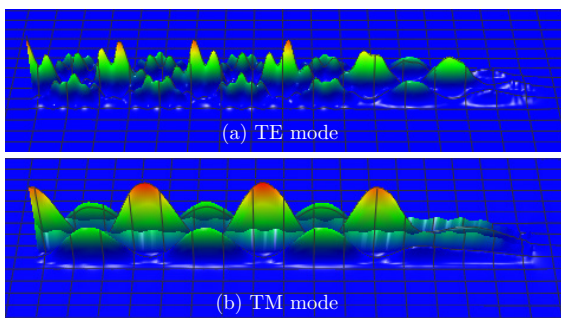


Fig. 7. Magnitude distribution of Poynting vector for three waveguides

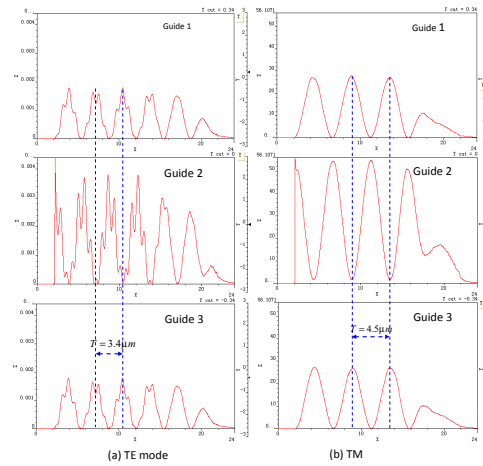


Fig. 8. Wave profiles in silicon waveguide.

coupled into guide 1 and guide 3 is obviously lower than that of the guide 2 due to the absorption by material, beam scattering, and the transmitting loss, etc.

In order to avoid coupling back again between adjacent waveguides, the tree-shaped structure is considered in our design, in which the spacing between the neighbor output ports is 2 μm as shown in Fig. 1. Moreover, considering decrease in the power difference of the three output ports, the total length of 1 × 3 BS is about 7 μm. Consequently, the signals are transmitted along their own waveguide channels and they do not interfere with each other.

The magnitude of Poynting vector distribution and  $H_y$  of TM polarization are given in Figs. 9(a) and (b), respectively. When the incident power is normalized to 1, the coupling powers of the output ports 1, 2, and 3 at a wavelength of 1.55 μm are 20%, 34%, and 18%, respectively. The ratio of the total output power, including three output ports, to the incident power is equal to 72%. The maximum power difference among three output ports is obviously equal to 16%.

The wavelength bandwidth, which is also discussed in our design, is shown in Fig. 10, where the total power represents the ratio of total coupling power of three output ports to the incident power, and the difference value denotes the maximum power difference for three output ports.

Figure 10 indicates that the total power is higher than 60%. Simultaneously, the difference value is less than 10% when wavelength is changed from 1.492 to 1.542 μm. In particular, the output power at port 1 is nearly equal to that at port 3 due to symmetrical

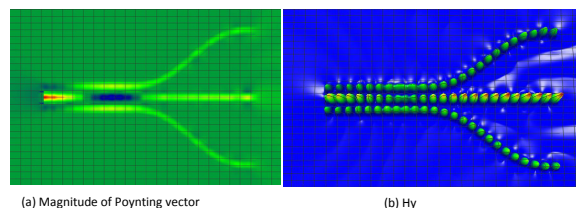


Fig. 9. Optical field distribution of 1 × 3 BS.

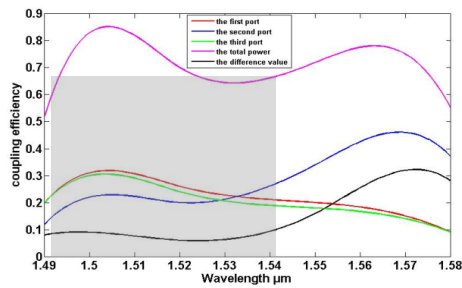


Fig. 10. Coupling efficiency as a function of wavelength.

waveguide structure and identical design parameters. Consequently, the wavelength bandwidth is about 50 nm in this case, which can realize nearly equal power splitting and enough for practical applications.

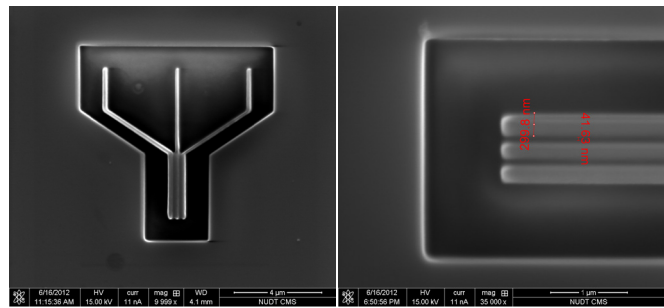
It is observed that the TE polarization is the same to above discussion. For simplification, the detailed discussions are omitted in this paper.

Figures 11(a) and (b) correspond to Scanning Electron Microscope (SEM) pictures of  $1 \times 3$  BS, which is fabricated using the Heos Li Nanoalb<sup>TM</sup> 600i of FEI company, including Focused Ion Beam and SEM<sup>[13]</sup>. The width of waveguide and the gap between neighbor waveguide are 299.8 nm and 41.63 nm, respectively.

As it is well-known that focused ion beam lithography is used to fabricate the device, the Gallium ions tend to dope into the silicon waveguide resulting in dramatically large absorption. Thus, the electron beam lithography and dry etching method are considered to fabricate the sample in the following experiments.

It is observed that the signal beam is coupled with grating couplers, which are fabricated on two ends of the sample. The input and output fibers are mounted on high-precision 3-axis translation stages. By using custom adapter plates, the fibers can be mounted vertically. The sample is mounted on a vacuum chuck on a two-axis stage. The input fiber is connected to a tunable laser, whereas the output fiber is connected to a power detector to measure the transmitted power. Both the laser and detector are connected to a PC using the GPIB interface. An alternative method is to use a fiber to couple light, and to measure the output power at a cleaved facet. At the output side, a microscope objective is used to collect the light from the output facet. This light is imaged onto a power detector or an infrared camera. The objective is mounted on a 3-axis translation stage. During the initial alignment, the infrared camera is used to monitor the light coming from the facet. When the objective lens is properly aligned, the output light is focused on the power detector and the power transmission is measured. Further research results will be proposed in near future.

In conclusion, we propose and demonstrate numerically a compact  $1 \times 3$  BS based on three parallel planar waveguides at a wavelength bandwidth of 50 nm (from 1.492 to 1.542  $\mu\text{m}$ ). We use FDTD method for optimization and numerical characterization of the device. Simultaneously, relative high-power efficiency beyond 60% and low power



(a) BS nanostructures (b) the expanded local image

Fig. 11. SEM pictures of  $1 \times 3$  beam splitter.

difference (10%) among three output branches of waveguide are achieved by this device. In principle, the energy distribution on the two outside waveguides should be identical for the symmetric shape of the  $1 \times 3$  BS. However, the power difference of two output waveguides is due to coarse mesh size, design error, such as waveguide length, width and the angle of tree-shaped waveguide, etc. Consequently, there is a discrepancy in theory design and simulation results. The  $1 \times 3$  BS is easy to fabricate using a single etching step and to integrate with other photoelectronic devices. Moreover, our splitter is placed anywhere on a chip because it allows planar coupling and splitting, which makes the system design more flexible.

This work was supported by the National Natural Science Foundation of China (60907003), the Foundation of NUDT (JC13-02-13), the Hunan Provincial Natural Science Foundation of China (13JJ3001), and Program for New Century Excellent Talents in University. The authors gratefully acknowledge helpful discussions with Prof. Zhiping Zhou and Dr. Junbo Feng.

## References

1. J. Yang, Z. Zhou, W. Zhou, X. Zhang, and H. Jia, *IEEE Photon. Technol. Lett.* **23**, 896 (2011).
2. J. Feng, C. Zhou, J. Zheng, and B. Wang, *Opt. Commun.* **281**, 5298 (2008).
3. R. Schnabel, A. Bunkowski, O. Burmeister, and K. Danzmann, *Opt. Lett.* **31**, 658 (2006).
4. M. Zhang, R. Malureanu, A. C. Kruger, and M. Kristensen, *Opt. Express* **18**, 14944 (2010).
5. W. Y. Liang, J. W. Dong, and H. Z. Wang, *Opt. Express* **15**, 1234 (2007).
6. X. Zhang and A. M. Armani, *Opt. Lett.* **36**, 3012 (2011).
7. N. Nozhat and N. Granpayeh, **4**, 1 (2010).
8. W. K. Burns and A. F. Milton, *Waveguide transitions and junctions in Guided-Wave Optoelectronics*, 2nd edn, T. Tamir (ed.) (Springer, Berlin, Heidelberg, 1990).
9. A. Yariv, *IEEE J. QE-9*, 919 (1975).
10. A. Yariv, *Quantum Electronics*, 3rd edn (Wiley, New York, 1989).
11. R. G. Hunsperger, *Integrated Optics* (Springer Science + Business Media, LLC, 2009).
12. B. E. A. Saleh and M. C. Teich, *Fundamentals of Photonics*, 2nd edn (Wiley). New York, 1991.
13. www.feicompany.com